

Supporting Information for:

Low voltage and hysteresis-free blue phase liquid crystal dispersed by ferroelectric nanoparticles

Ling Wang,^a Wanli He,^a Xia Xiao,^c Man Wang,^a Meng Wang,^a Pangyen Yang,^c Zhangjian Zhou,^a Huai Yang,*^{a,b} Haifeng Yu*^b and Yunfeng Lu*^d

^a School of Materials Science and Engineering, University of Science and Technology Beijing, Beijing 100083, P. R. China. Fax: +86-10-62333969; Tel: +86-10-62333969; E-mail: yanghuai@mater.ustb.edu.cn (H. Yang)

^b Department of Materials Science and Engineering, College of Engineering, Peking University, Beijing 100871, P. R. China. E-mail: yanghuai@coe.pku.edu.cn (H. Yang); yuhaifeng@pku.edu.cn (H. Yu)

^c AU Optronics Trade (Shanghai) Corporation, Suzhou 215021, P. R. China.

^d Department of Chemical and Biomolecular Engineering, University of California, Los Angeles, CA 90095, USA. E-mail: luucla@ucla.edu (Y. Lu)

Preparation of the Nanoparticles.^[1,2,3]

Preparation of ferroelectric nanoparticles: The ferroelectric BaTiO₃ nanoparticles were prepared by milling large particles (~1 μm in size), which were mixed with a solution of oleic acid (surfactant) in heptane in a weight ratio of 1:2:10, respectively, then the particles were ground in a planetary ball mill for 15 hours. The morphology and particle sizes of the sample were characterized by JEM-100CXII transmission electron microscopy (TEM) operated at 100 kV. A small amount of the powder products was dispersed in heptane and placed in an ultrasonic bath to make a suspension, and then a droplet of the solution was transferred onto a carbon-coated copper grid for the TEM observation. **Figure S1** shows TEM image of the BaTiO₃ nanoparticles prepared by a high-energy milling process. As is shown, the BaTiO₃ particles have an average diameter of ~30 nm.

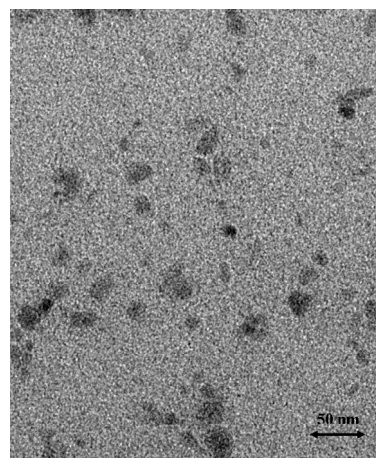


Figure S1. TEM image of the BaTiO₃ nanoparticles prepared by a high-energy milling process.

Preparation of non-ferroelectric nanoparticles: The hydrophobic surface-treated ZnS NPs with an average diameter of ~33 nm were synthesized in reversed micelle following standard procedures with a slight revision, using Triton X-100 as a surfactant. The preparation was carried out by mixing two reverse micellar solutions with the same water-to-surfactant molar ratio ($W_o = [W]/[S]$) containing the same concentration of Zn²⁺ or thioacetamide. To make a stable reverse micelle, a solution of ZnAc₂·2H₂O or thioacetamide was added into a mixture of cyclohexane and Triton X-100, followed by dropwisely adding a small amount of n-butanol as a co-surfactant under stirring. After the mixture became clear, a 1:1 molar ratio of zinc-ion-containing micelle mixed with sulfur-containing micelle, stirred with the aid of ultrasound for the desired time, yields a yellowish emulsion. The XRD spectrum and TEM image of the ZnS NPs have been reported by our previous work.^[3]

Preparation of the Samples.

The BPI-exhibiting LC materials (BPLC) was a mixture comprising the following materials: SLC-X (82.0 wt%, Yongsheng Huatsing Liquid Crystal Co., Ltd, $\Delta n = 0.235$, $\Delta \epsilon = 29.6$ at 298 K), R811 (10.0 wt%, Merck) and Iso-(6OBA)₂ (8.0 wt%, synthesized by our laboratory), the molecular structures of chiral dopants are shown in **Figure S2**. And the liquid crystalline composites doped with different concentrations of the non-ferroelectric or ferroelectric NPs were prepared by dispersing the NPs into BPLC. In order to achieve good dispersion, the mixtures of BPLC with the NPs were dissolved in heptane and sonicated for about 1.0 h. Then, heptane was evaporated off slowly for about 24 h above 45 °C before the samples were placed in a vacuum system at 1023 Torr for 24 h at 50 °C. At last, the mixture was ultrasonically dispersed for 5 min before it was injected into IPS cell. The actual phase transition temperatures of the liquid crystalline composites doped with different concentrations of ZnS or BaTiO₃ NPs were listed in **Table S1**. The initial phase assignments and corresponding transition temperatures for the composites were determined by using the thermal optical microscopy with a polarizing microscope (Olympus BX-51), and the temperature was controlled with a hot stage calibrated to an accuracy of ± 0.1 °C (Linkam LK-600PM). The physical parameters of host nematic LCs doped with different concentrations of ZnS or BaTiO₃ NPs, which have been checked at 298K, are summarized in **Table S2**.

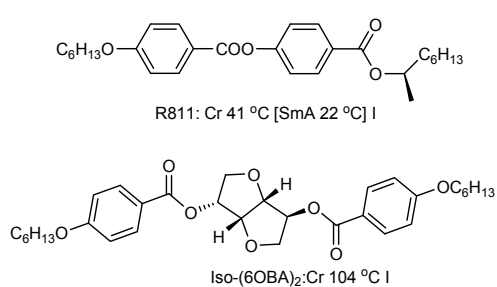


Figure S2. Molecular structures of chiral dopants

Table S1. The composition and transition temperatures of neat BPLC and ZnS or BaTiO₃ NPs dispersed BPLCs.

BPLC/ wt%	Nanoparticles / wt%	Temp. range / °C	
		ZnS	BaTiO ₃
100.0	0.0	55.0-45.0	55.0-45.0
99.9	0.1	56.4-44.4	55.8-44.5
99.7	0.3	57.2-43.0	57.0-43.2
99.5	0.5	56.8-41.2	59.3-42.6
99.3	0.7	56.6-42.4	60.5-44.0
99.0	1.0	56.0-44.2	62.0-48.2
98.5	1.5	55.4-46.7	63.4-53.9

Table S2. Observed physical parameters of host nematic LC dispersed by ZnS or BaTiO₃ NPs at 298 K.

SLC-X/ wt%	Nanoparticles / wt%	ZnS		BaTiO ₃	
		Δn	Δε	Δn	Δε
100.0	0.0	0.235	29.6	0.235	29.6
99.9	0.1	0.235	29.9	0.235	30.5
99.7	0.3	0.237	30.1	0.240	32.1
99.5	0.5	0.236	30.7	0.237	35.9
99.3	0.7	0.238	31.8	0.243	38.3
99.0	1.0	0.237	33.9	0.248	41.7
98.5	1.5	0.239	35.6	0.251	45.2

Measurement of Electric-Induced Birefringence.^[4,5]

Figure S3 depicts the schematic diagram of the experimental set-up for measuring the birefringence induced by an electric field. The samples in the in-plane-switching (IPS) cells were perpendicularly placed with respect to the incident light. **Figure S4** shows the photos of the actual experimental set-up in AU Optronics Trade Corporation. The temperature was controlled with a hot stage calibrated to an accuracy of ± 0.1 °C (Linkam LK-600PM) by a proportional integral differential (PID) controller. To measure the electric-induced birefringence, an alternating current (AC) rectangular field of 60 Hz supplied by a power amplifier and a function generator was applied between the electrodes in the IPS cell. The transmitted light intensity through the cell placed between crossed polarizers was detected by a photodiode. The second harmonic component of the output ac signal from the photodiode was recorded with a digital storage oscilloscope. Herein, the IPS cells were kindly supplied by AU Optronics Corporation, and the indium tin oxide electrode width was 5.0 μm , the distance between the electrodes was 5.0 μm , and the cell gap was maintained at 10.0 μm by spacers.

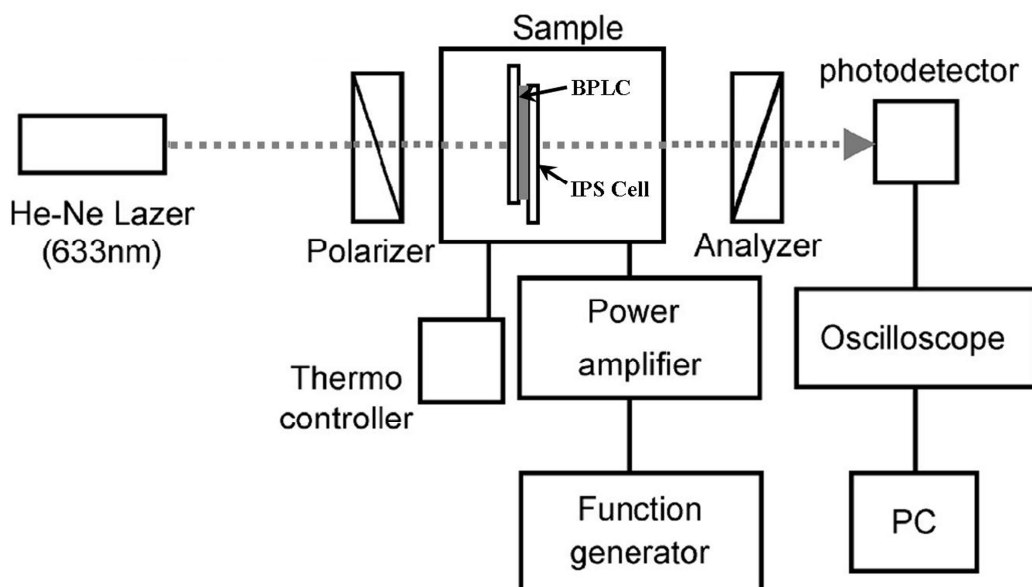


Figure S3. Experimental set up for birefringence measurement.

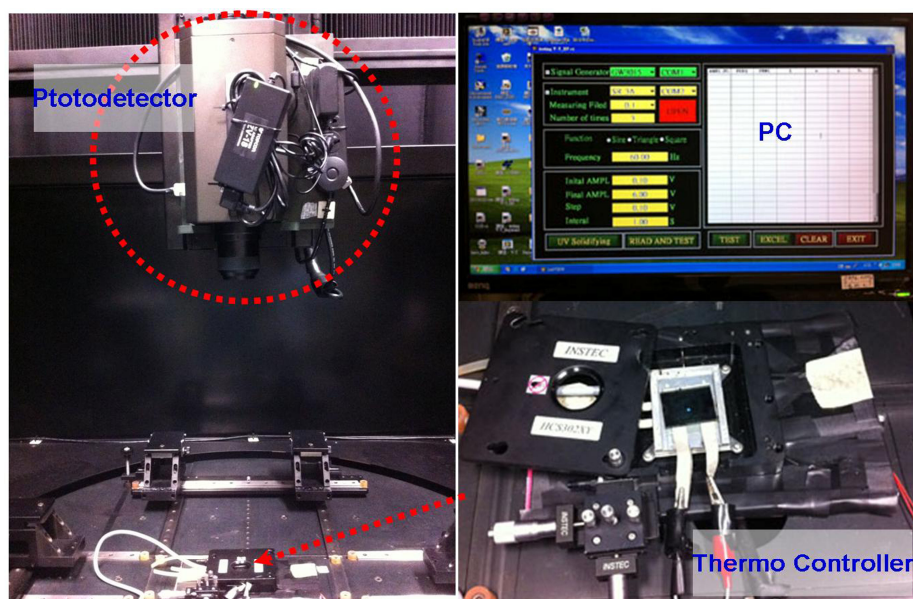


Figure S4 The photos of the actual experimental set-up in AU Optronics Trade Corporation.

The change in output intensity due to optical retardation generated by an applied electric field was measured. Output intensity I_{out} is expressed by Eq. (1):

$$I_{\text{out}} = I_{\text{in}} \sin^2(\phi/2) \quad (1)$$

where I_{in} is the input intensity and ϕ is the optical retardation which can be determined by measuring the ratio $I_{\text{out}}/I_{\text{in}}$, correspondingly. The observed change in birefringence Δn is calculated from Eq. (2):

$$\phi = 2\pi\Delta nL/\lambda \quad (2)$$

where L is the length of the light path. i.e., the cell gap between the bottom and top substrates.

Macroscopically, BPLC is an isotropic Kerr medium when there is no external electric field (E) present. As E increases, the BPLC becomes anisotropic along the electric field direction, and the change of the refractive index follows the Kerr effect in the low field region but gradually saturates as the electric field keeps increasing, which can be well explained by an extended Kerr effect. Based on the Kerr effect, the induced birefringence $\Delta n_{induced}$ in the weak field region is related to E , wavelength λ , and Kerr constant K as:

$$\Delta n_{induced} = \lambda KE^2 \quad (3)$$

Calculation of the Kerr Constant K .^[5,6]

Based on the data from the measurement of electric-induced birefringence, we can get the plot for the electric birefringence of BPLC a function of the square of the applied electric field, and the electric birefringence is approximately proportional to the square of the electric field, i.e., the equation for the Kerr law Eq. (3) is followed and the slope indicates the Kerr constant.

Figure S5 illustrates the variation of induced birefringence with square of an applied electric field in the BPLC doped with 0.5 wt% ZnS nanoparticles at the reduced temperature T , $T_{l-BP} - T = 6.0$ °C. From the slope, we can get the Kerr constant: $\sim 1.25 \times 10^{-9}$ mV⁻². **Figure S6** shows the Kerr constant in the BPLC dispersed by different concentrations of ZnS or BaTiO₃ NPs.

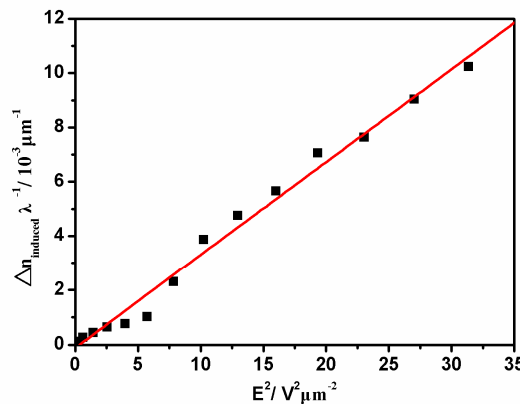


Figure S5. Variation of induced birefringence with square of an applied electric field for

BPLC doped with 0.5 wt% ZnS nanoparticles at the reduced temperature T , $T_{\text{I-BP}} - T = 6.0 \text{ }^{\circ}\text{C}$.

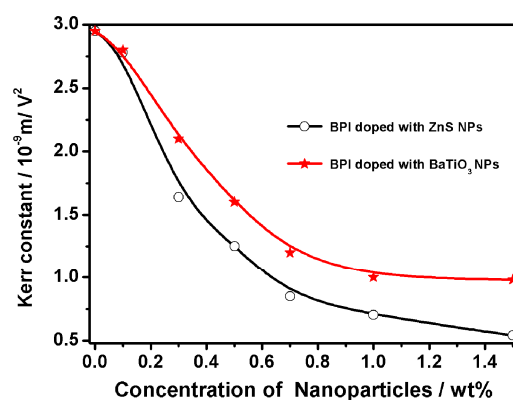


Figure S6. The Kerr constant in the BPLC dispersed by different concentrations of ZnS or BaTiO₃ NPs.

Calculation of the Device Parameter A .^[7,8]

The driving voltage (on-state voltage, V_{on}) is closely related with the Kerr constant of materials and the electrode configuration of devices, which can be expressed as follow:

$$V_{\text{on}} = \frac{A}{\sqrt{K}} \quad (4)$$

where A is a device parameter which is affected by the electrode configuration, and K is the Kerr constant of materials.

In order to calculate the device parameter A , we obtain the on-state voltage and Kerr constant at different temperatures for each sample and then plot V_{on} against $1/\sqrt{K}$, where the slope indicates device parameter A . **Figure S7** depicts the variation of V_{on} with $1/\sqrt{K}$ at different temperature for BPLC doped with 0.5 wt% ZnS nanoparticles. From the slope, we can get the device parameter A : $\sim 2.48 \text{ } \mu\text{m}^{1/2}$. **Figure S8** shows the device parameter A in the BPLC dispersed by different concentrations of ZnS or BaTiO₃ NPs.

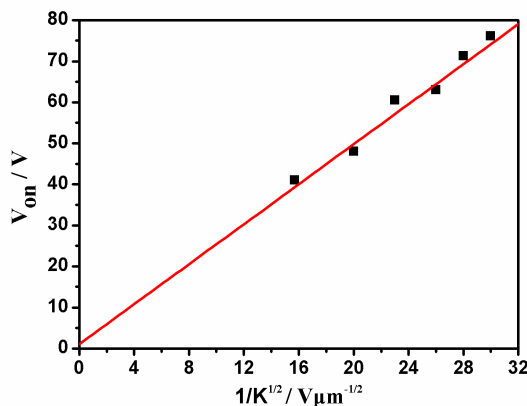


Figure S7. Variation of the V_{on} with $1/\sqrt{K}$ at different temperature for BPLC doped with 0.5 wt% ZnS nanoparticles.

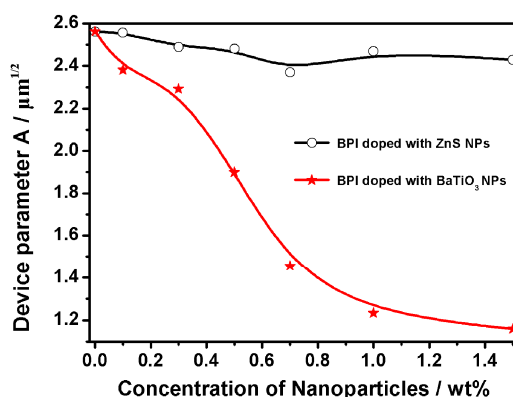


Figure S8. The device parameter A in the BPLC dispersed by different concentrations of ZnS or BaTiO₃ NPs.

Response Times of the BPLC.

The response time for the rise process is defined as $t_{0-90}(t_{on})$, which is the time for the increase in the transmittance from the initial state to 90% of the saturated state. That for the decay process is defined as $t_{100-10}(t_{off})$, which is the time for the decrease in the transmittance from the initial state to 10% of the saturated state. **Table S3** shows the response time (t_{on} , t_{off}) for the BPLC doped with different concentration of ZnS or BaTiO₃ at the reduced temperature T , $T_{I-BP} - T = 6.0$ °C.

Table S3. The response time (t_{on} , t_{off}) for the BPLC doped with different concentration of ZnS or BaTiO₃ at the reduced temperature T , $T_{l-BP} - T = 6.0$ °C.

Nanoparticles	Response Time / ms	Concentration of Nanoparticles / wt%				
		0	0.3	0.5	0.7	1.5
ZnS	t_{on}	0.48	0.51	0.53	0.55	0.60
	t_{off}	-	0.5	0.45	0.43	0.42
BaTiO ₃	t_{on}	0.48	0.47	0.45	0.46	0.50
	t_{off}	-	0.45	0.4	0.4	0.44

References for Supporting Information

- [1] A. Schurian and K. Barner, *Ferroelectr. Lett. Sect.* **1996**, *20*, 169.
- [2] H. Atkuri, G. Cook, D. R. Evans, C. I. Cheon, A. Glushchenko, V. Reshetnyak, Y. Reznikov, J. L. West and K Zhang, *J. Opt. A: Pure Appl. Opt.* **2009**, *11*, 024006.
- [3] L. Wang, C. Zhao, F. Meng, S. Huang, X. Yuan, X. Xu, Z. Yang and H. Yang, *Colloids and surfaces A: Physicochem. Eng. Aspects* **2010**, *360*, 205.
- [4] L. M. Sabirov and D. I. Semenov, *Opt. Spectrosc.* **2006**, *101*, 299.
- [5] Y. Haseba and H. Kikuchi, *J. Soc. Info. Display* **2006**, *14*, 551.
- [6] M. Lee, S. T. Hur, H. Higuchi, K. Song, S. W. Choi and H. Kikuchi, *J. Mater. Chem.* **2010**, *20*, 5813.
- [7] L. Rao, J. Yan, S. T. Wu, S. Yamamoto and Y. Haseba, *Appl. Phys. Lett.* **2011**, *98*, 081109.
- [8] L. Rao, Z. Ge, S. T. Wu and S. H. Lee, *Appl. Phys. Lett.* **2009**, *95*, 231101.